ACS Partner Journal
PRECISION CHEMISTRY

pubs.acs.org/PrecisionChem
Article

Tetravalent Terbium Chelates: Stability Enhancement and Property Tuning

Tianjiao Xue, You-Song Ding,* Xue-Lian Jiang, Lizhi Tao, Jun Li, and Zhiping Zheng*

Cite This: *Precis. Chem.* 2023, 1, 583−591
Read Online

ACCESS | Metrics & More | Article Recommendations | Supporting Information

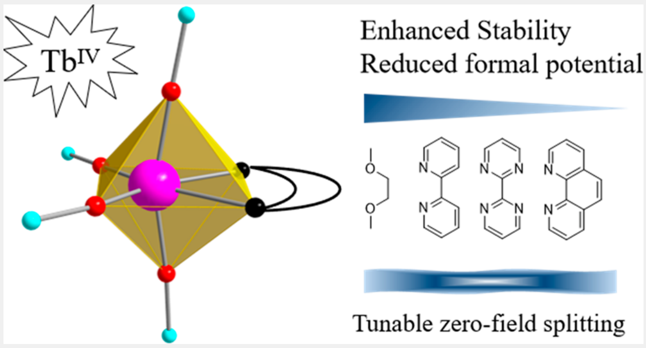

ABSTRACT: Coordination chemistry of rare-earth elements has been dominated by the +3 oxidation state. Complexes with higher-valence lanthanide ions are synthetically challenging but are of fundamental research interest and significance as advanced molecular materials. Herein, four tetravalent terbium complexes (**2**−**5**) of the common formula $[Tb(OSiPh_3)_4L]$ (L = ethylene glycol dimethyl ether (DME), 2,2′-bipyridine (bpy), 2,2′-bipyrimidine (bpym), and 1,10-phenanthroline (phen)) are reported. Crystallographic analyses reveal in each of these complexes a hexacoordinate Tb(IV) ion situated in a distorted octahedral coordination environment formed by four triphenylsiloxido ligands and a bidentate chelating ligand. The use of chelating ligands enhances the stability of the resulting complexes over their THF solvate precursor. More significantly, the aromatic N-chelating ligands have been found to tune effectively the electronic structures of the complexes, as evidenced by the sizable potential shifts observed for the quasi-reversible redox Tb(IV/III) process and by the changes in their absorption spectra. The experimental findings are augmented with quantum theoretical calculations in which the ligand π-donation to the 5*d* orbitals of the Tb(IV) center is found to be primarily responsible for stability enhancement and the corresponding changes of physical properties observed. Magnetic measurements and results from electron paramagnetic resonance studies produced small absolute values of zero-field splittings of these complexes, ranging from 0.1071(22) to 1.1484(112) cm^{-1} and comparable to the values reported for analogous Tb(IV) complexes.

KEYWORDS: *Tetravalent Terbium Ion, Chelating Ligand, Formal Potential, Stability, Magnetic Property*

■ INTRODUCTION

Complexes with their metal ions in unusual oxidation states are of interest for fundamental research and applications of practical significance. For example, high-valence iron species play a major role in oxidative reactions in nature,[1] while actinide ions in their unconventionally high oxidation states enable their effective separation from a gamut of coexisting rare earth ions.[2,3] In this context, the coordination chemistry of the lanthanide (Ln) ions in unconventional oxidation states is of particular relevance and of high interest to researchers interested in theoretical and computational chemistry, synthetic and structural chemistry, physical properties and chemical reactivity, and materials applications of the lanthanides. However, the chemistry of the lanthanides is dominated by the +3 oxidation state, with the few exceptions of Ce(IV), Sm(II), Eu(II), and Yb(II) being reasonably readily accessible.[4−10] With the pioneering work by Lappert and co-workers[11] and the following efforts by Evans, Mazzanti, Meyer, Long, and others, remarkable progress in the chemistry of Ln(II) ions has been achieved.[12−27] The isolation of divalent complexes of all lanthanide elements was completed in 2013,[23] some of which display intriguing physical properties with potential applications as high-performing single-molecule magnets[26] and molecular spin qubits.[27] In stark contrast, the chemistry of high-valence lanthanide ions has lagged far behind due primarily to the lack of synthetic methods or reagents and the notorious air/moisture sensitivity or reactivity of such high-valence species. In this context, the formation of Pr(V) species in the gas phase and in a solid noble-gas matrix is noteworthy.[28,29] It is also of note that the Tb(IV) ion in the solid was identified more than 70 years ago,[30,31] but complexes of tetravalent lanthanide other than Ce(IV) were unknown until very recently. It is the efforts led independently by Mazzanti[32−35] and La Pierre[36−38] that have broken new ground in the chemistry of tetravalent lanthanide complexes.[39]

A number of representative Tb(IV) complexes are collected in time order as shown in Scheme 1, the first being $[Tb(OSi(O^tBu)_3)_4]$ (**A**) reported by Mazzanti and co-workers

Received: June 9, 2023
Revised: September 8, 2023
Accepted: September 11, 2023
Published: October 2, 2023

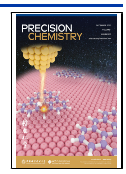

Scheme 1. Structures of the Tb(IV) Complex in the Literature[a]

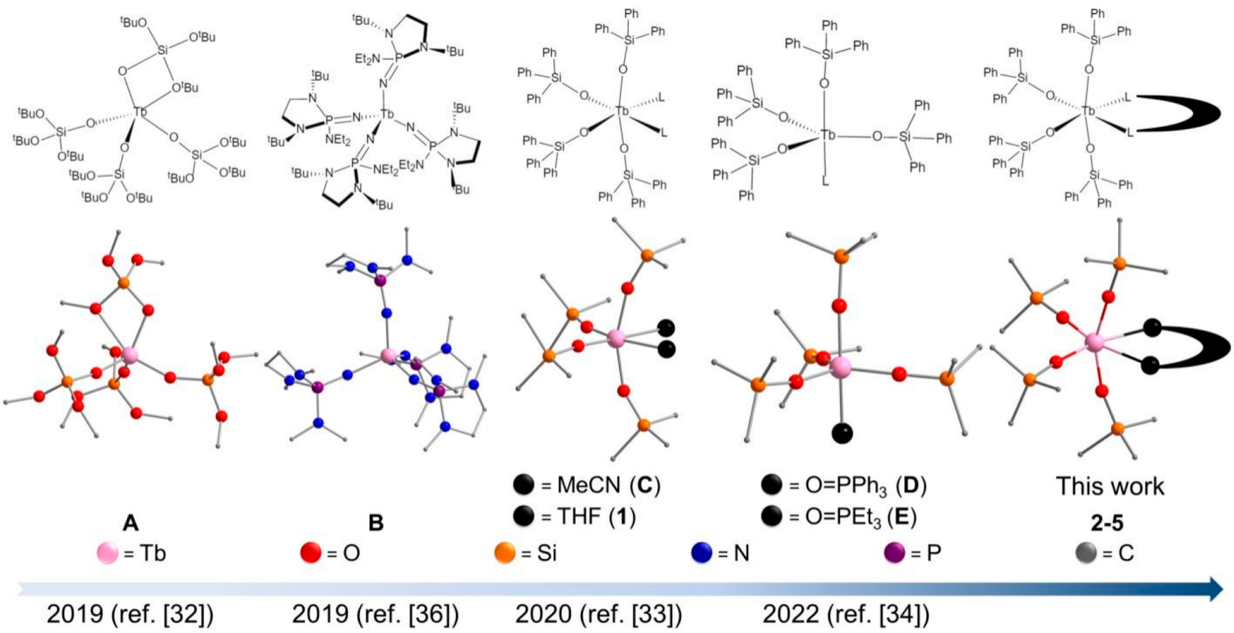

[a]The rightmost one represents the generic structure of the chelates in this work.

with its pentacoordinate Tb(IV) center situated in a coordination sphere formed by four $OSi(O^tBu)^-$ ligands.[32] La Pierre et al. reported $[Tb(NP(1,2\text{-bis-}^tBu\text{-diamidoethane})(NEt_2))_4]$ (**B**) stabilized by phosphinimine ligands (PN*) in the same year.[36,37] Shortly after, Mazzanti and co-workers reported the first Pr(IV) complex $[Pr(OSiPh_3)_4(MeCN)_2]$[35] by adopting the same procedure for the preparation of its Tb(IV) congeners $[Tb(OSiPh_3)_4(L)_2]$ (L = CH_3CN (**C**) or THF (**1**)) and $[Tb(OSiPh_3)_4(L)]$ (L = O=PPh_3 (**D**) or O=PEt_3 (**E**)).[33,34] Out of the small number of tetravalent lanthanide complexes, these of Pr(IV) and Tb(IV), featuring, respectively, $4f^1$ and $4f^7$ electron configurations, are magnetically attractive, both capable of providing a pure nuclear-spin environment and hyperfine coupling between nuclear and electronic spins. Potential applications as single-molecule magnets and molecular spin qubits can be envisioned.[40−44] It is thus important to develop tetravalent Pr(IV) and Tb(IV) complexes with enhanced stability and to study their physicochemical properties with an eye on the aforementioned applications.

Ligand substitution was studied by Mazzanti and co-workers who found that the coordinated solvent molecules in $[Tb(OSiPh_3)_4(L)_2]$ (L = CH_3CN or THF) can be replaced by phosphinoxide ligands,[33,34] leading to the enhanced stability of the resulting complexes due to the strong π(O−Tb) interaction from phosphinoxide ligands. Inspired by these literature reports and in hopes of producing tetravalent lanthanide complexes with even further enhanced stability for property studies, we explore in this work the replacement of the coordinated tetrahydrofuran (THF) molecules in $Tb(OSiPh_3)_4(THF)_2$ (**1**)—one of the early examples of Tb(IV) complexes—with a number of O- and N-chelating ligands. Specifically, the syntheses and crystal structures of four new tetravalent Tb(IV) complexes (**2**−**5**, Scheme 2) are reported, with each featuring four triphenylsiloxido ligands and a bidentate chelating ligand, including ethylene glycol dimethyl ether (DME), 2,2′-bipyridine (bpy), 2,2′-bipyrimidine (bpym), and 1,10-phenanthroline (phen). Property studies by cyclic voltammetry, absorption spectroscopy, and DFT calculations reveal enhanced stability of the chelates over the precursor complex with two coordinated THF molecules and collectively point to the stabilizing effect of the chelating ligands. Magnetic measurements and studies by electron paramagnetic resonance (EPR) spectroscopy indicate that the absolute values of zero-field splitting for these complexes are relatively small.

Scheme 2. Syntheses of 2−5 by Ligand Exchange of $Tb(OSiPh_3)_4(THF)_2$ (1) with the Chelating Ligands Shown

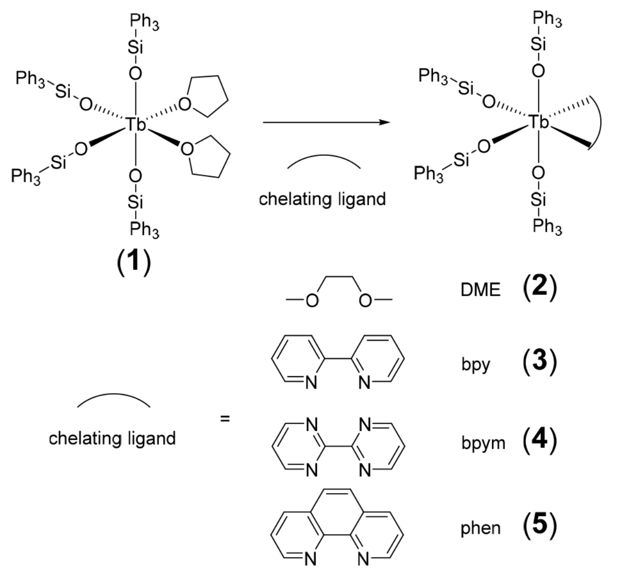

RESULTS AND DISCUSSION

Syntheses and Structural Characterization

Complex **1** was obtained by adopting a literature procedure:[34] Oxidizing the trivalent precursor $Tb(OSiPh_3)_3(THF)_3$ ($\mathbf{Tb^{Ph3}}$)[45] with $[(C_6H_4Br)_3N][SbCl_6]$ in the presence of $KOSiPh_3$, followed by recrystallization from THF at −30 °C,

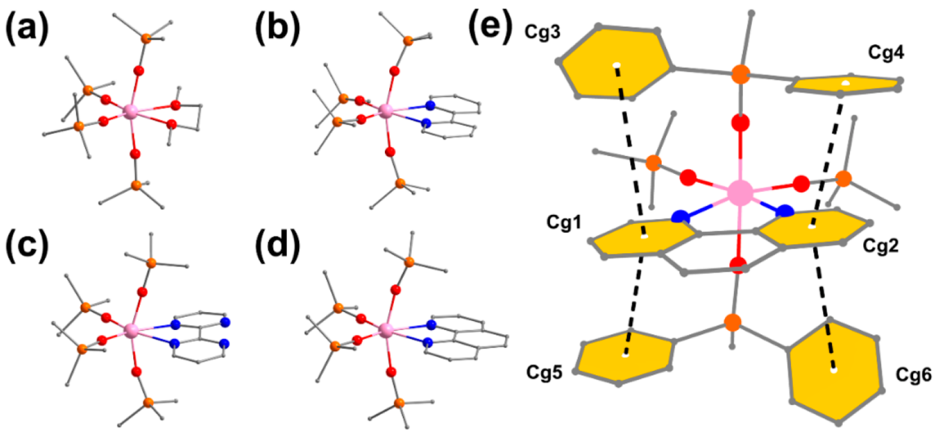

Figure 1. Stick-and-ball depiction of the crystal structures of (a) **2**, (b) **3**, (c) **4**, and (d) **5**, other atoms are omited for clarity; (e) $\pi-\pi$ interactions between the phenyl groups of the axial siloxido ligands and the aromatic rings of the phen ligand in **5**; yellow hexagons highlight the aromatic groups involved (color code: Tb, pink; O, red; Si, orange; C, gray; N, blue).

afforded the desired product. $LiOSiPh_3$ or $NaOSiPh_3$ can be used in place of $KOSiPh_3$, but the desired tetravalent complex was not formed without this additional equivalent of siloxido to balance the extra positive charge of the newly generated Tb(IV).[33,34] Complexes **2**−**5** were obtained by ligand exchange of **1** with its coordinated THF being replaced by DME, bpy, bpym, and phen, respectively (Scheme 2).

The solid-state structures of the four new complexes were established by single-crystal X-ray diffraction studies (Table S1). As shown in Figure 1, each of the four new complexes features a hexacoordinated Tb(IV) ion situated in a distorted octahedral coordination sphere formed by four Ph_3SiO^- ligands and a unique bidentate chelating ligand. Overall, these new complexes are structurally similar to the previously reported **1**[34] and $[Tb(OSiPh_3)_4(CH_3CN)_2]$ (**C**)[33] with two *cis*-disposed non-siloxido ligands. Except for solvent molecules of recrystallization, no ions of any kind are present in the complete crystal structure, which is consistent with the complexes being electrically neutral. Bond lengths and angles of interest are summarized in Table 1. The $Tb-O_{siloxido}$ bonds of the new complexes are comparable with these of the Tb(IV) complexes previously reported,[32−34] but shorter than these of the trivalent precursor $\mathbf{Tb^{Ph3}}$. Ranging from 65.09(4)° to 66.87(14)°, the O−Tb−O or N−Tb−N angles associated with the chelating ligands in **2**−**5** are significantly smaller than the $O_{THF}-Tb-O_{THF}$ angle in **1** (86.10(12)°), due presumably to the enhanced rigidity of the bidentate chelating ligands. Correspondingly, the angles between the two siloxido ligands that are coplanar with the chelating ligands, ranging from 100.10(4)° to 108.13(10)°, are significantly larger than the corresponding angle of 96.02(11)° in **1** (Table S2). This scenario is entirely understandable as the less crowded coordination of the chelating ligand makes room for a more relaxed disposition of the coplanar siloxido ligands. The remaining two siloxido ligands are "steered away" due to steric repulsion by the equatorial siloxido ligands, resulting in a pronounced deviation of the axial coordination motif from linearity (157.14(12)° to 165.07(10)°) (Table S2). Two phenyl groups on each of the axial siloxido ligands are disposed in such a way that strong face-to-face $\pi-\pi$ interactions are formed with the aromatic rings of the N-chelating ligand (Figures 1e, S1, S2; Tables S3−S5) The distortion of the coordination geometry from a perfect octahedron was estimated by continuous shape measures analysis[46] to be 0.654, 1.041, 1.297, 1.330, and 1.185 for **1**−**5**, respectively (Table S6). Albeit small, such deformation of the coordination polyhedra can perturb the electronic structure of a lanthanide complex, leading to significant changes in magnetic properties.[47,48]

Table 1. Selected Bond Lengths (Å) and Angles (deg) of $\mathbf{Tb^{Ph3}}$ and 1−5

	$Tb-O_{siloxido}$	Tb−O/N (L)[a]	O/N (L)−Tb−O/N (L)
$\mathbf{Tb^{Ph3}}$	2.135(3)−2.145(3)	2.441(3)−2.484(4)	
1	2.043(2)−2.079(2)	2.400(2)	86.10(12)
2	2.032(3)−2.084(3)	2.439(3)−2.443(3)	66.81(11)
3	2.039(4)−2.094(4)	2.462(5)−2.473(4)	65.38(14)
4	2.027(1)−2.078(1)	2.497(1)−2.503(1)	65.09(4)
5	2.044(2)−2.085(2)	2.461(3)	66.87(14)

[a]O/N (L) indicates the coordinating atoms (O in **1** and **2**; N in **3**−**5** of the neutral ligand L).

Cyclic Voltammetry

Redox properties of the complexes were studied by cyclic voltammetry (CV). The voltammograms are each characterized by a single pair of redox events, exhibiting a quasi-reversible redox process. As shown by the data collected in Table 2 (Figure 2), the reduction (E_{pc}) and oxidation (E_{pa}) potentials both decrease upon chelation of the Tb(IV) center, with the peaks shifting from 0.020 and 0.582 V of **1** to −0.278 and 0.078 V for **5**, respectively. The E_{pa} of 0.078 V for **5** is the smallest among all Tb(IV) siloxido complexes, and is only higher than that of **B**, a tetravalent terbium complex with a ligand of strong π character.[32−34,36]

Table 2. Electrochemical Data for the Tb(III/IV) Peak Couple of 1−5 vs Fc/Fc^+ (Fc = Ferrocene) in dichloromethane at a Sweep Rate of 500 mV s^{-1}

Complex	E_{pc} (V)	E_{pa} (V)	$E°$ (V)	ΔE (V)	I_{pa}/I_{pc}
1	0.020	0.582	0.301	0.562	0.894
2	−0.017	0.346	0.165	0.363	0.996
3	−0.164	0.223	0.030	0.387	0.823
4	−0.208	0.266	0.029	0.474	0.792
5	−0.278	0.078	−0.100	0.356	1.093

https://doi.org/10.1021/prechem.3c00065
Precis. Chem. 2023, 1, 583−591

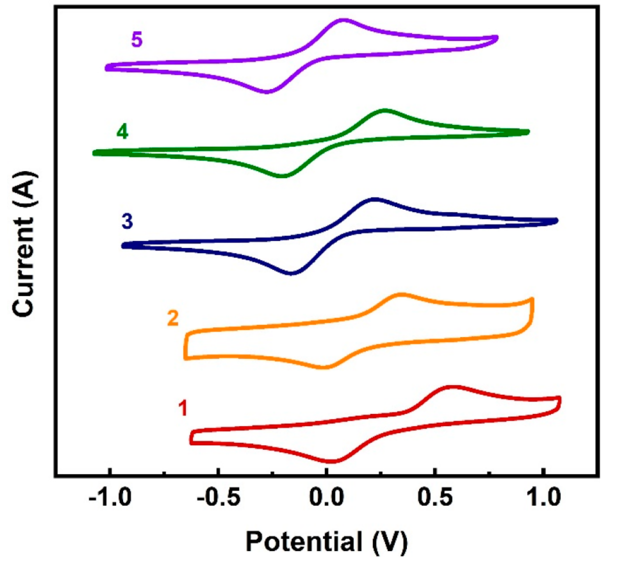

Figure 2. Cyclic voltammograms of **1**−**5** (1 mM in dichloromethane) with $[N^nBu_4][B(C_6F_5)_4]$ (0.1 mM) as supporting electrolyte at a sweep rate of 500 mV s^{-1} vs Fc/Fc^+.

The peak separations (ΔE) for **2**−**5** is smaller than that of **1** by about 0.1−0.2 V, and even smaller than these of the other previously reported Tb(IV) complexes (Table 2),[32−34,36] reflecting well the enhanced stability of the chelates during the redox process. The relationship between the peak current and the square root of the scan rate was found to be nearly linear, and the ΔE increased with increasing scan rate, suggesting that Tb(III/IV) redox reactions are diffusion-controlled. For **2**−**5**, the ratio of peak currents (I_{pa}/I_{pc}) ranges from 0.8 to 1.2, indicating that the reduced species were mostly reoxidized upon reversal of the scan direction, exhibiting good chemical reversibility (Figures S5−S12). In contrast, the peak current ratio of **1** varies more sensitively upon change of scan rate (Figures S3 and S4, Table S7). This result suggests that the redox process of **1** is more complex, possibly involving dissociation and recoordination of the THF ligands, a scenario corroborated by the large separation between the reduction and oxidation peaks observed for **1**.

The formal potential ($E°$), a good reflection of the relative thermodynamic stability of the Tb(IV) and Tb(III) redox states,[49−51] ranges from −0.1 V of **5** to 0.301 V of **1** (Table 2). In other words, the use of chelating ligands is propitious to enhancing the thermodynamic stability of a complex, which is completely expected. Soundly supporting this conclusion is the shift of $E°$ from 0.301 V for **1** to 0.165 V for **2** with the mere substitution of two coordinated THF molecules with a single DME ligand. It appears that introduction of a conjugated chelating ligand can further enhance the stability of the complex as reflected by the further reduced $E°$, to 0.030, 0.029, and −0.100 V for **3**−**5**, respectively (Table 2). Complex **5** emerged as the most thermodynamically stable among complexes **1**−**5**, probably owing to the additional conjugated phenyl ring relative to the 2,2′-bipyridine ligand.

UV−Vis Spectra

The UV−vis spectra of **1**−**5** were collected immediately following dissolution in toluene (Figure 3) and dichloromethane (Figure S13). The absorptions of **1** and **2** in toluene, spanning between 285 and 575 nm, show maxima at ca. 382 nm, while the absorptions of the N-chelates (**3**−**5**) covers the 320−550 nm range with maxima at ca. 371 nm. The spectra obtained with dichloromethane solutions are essentially the same as these with the toluene solutions with only a <5 nm shift of the absorption maxima (Table 3). The molar absorptions, ranging from 3300 to 4200 M^{-1} cm^{-1} for **1**−**5**, are comparable to the values reported for analogous Tb(IV) siloxido complexes[32−34] and an electrochemically generated Tb(IV) species.[52,53]

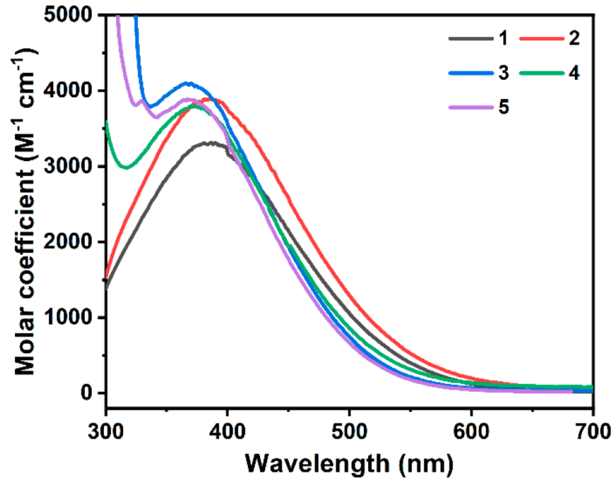

Figure 3. UV−vis absorption spectra of **1**−**5** in toluene at room temperature.

Table 3. Experimental and TDDFT Results (nm) of the Absorption Maxima for 1−5

Complexes	Dichloromethane	Toluene	Excitation energy	Assignments
1	382	385	388	LMCT
2	383	384	384	LMCT
3	370	370	378/373	LLCT/LMCT
4	374	373	377/375	LLCT/LMCT
5	370	370	376/374	LLCT/LMCT

To rationalize the blue shift of absorption maxima of the N-chelates (**3**−**5**) with respect to these of **1** and **2**, TDDFT calculations were performed, and the results are summarized in Tables 3 and S13.[54] The computed UV−vis spectra (Figure S15) are in excellent agreement with the experimental ones. The broad bands of **1** and **2** are attributed exclusively to the ligand-to-metal charge transfer (LMCT) from the ligand-dominant molecular orbitals (MOs) to the Tb 4*f* orbitals (Figure S16). In comparison, the absorption maxima of **3**−**5** can be characterized as a dominant LMCT with an appreciable ligand-to-ligand charge transfer (LLCT) contribution (Figure S17). Specifically, these LLCT peaks can be assigned to ligand-dominant $\pi \rightarrow \pi^*$ electronic transitions of these N-chelated ligands, leading to the blue-shifted absorption and demonstrating the stabilization of the π-orbitals upon coordination with the aromatic N-chelating ligand (Figure S18).[55]

The solution stability of the Tb(IV) complexes was evaluated with their UV−vis spectra collected over a period of 2 weeks in toluene (Figure 4) and 1 week in dichloromethane (Figure S14) under an argon atmosphere. In toluene, the solutions of **1** and **2** decolored completely after 72 h, whereas 39%, 17%, and 49% of the characteristic absorption were retained after 120 h for the solutions of **3**−**5**, respectively. The enhancement of solution stability of **3**−**5** can be attributed to the strong intramolecular

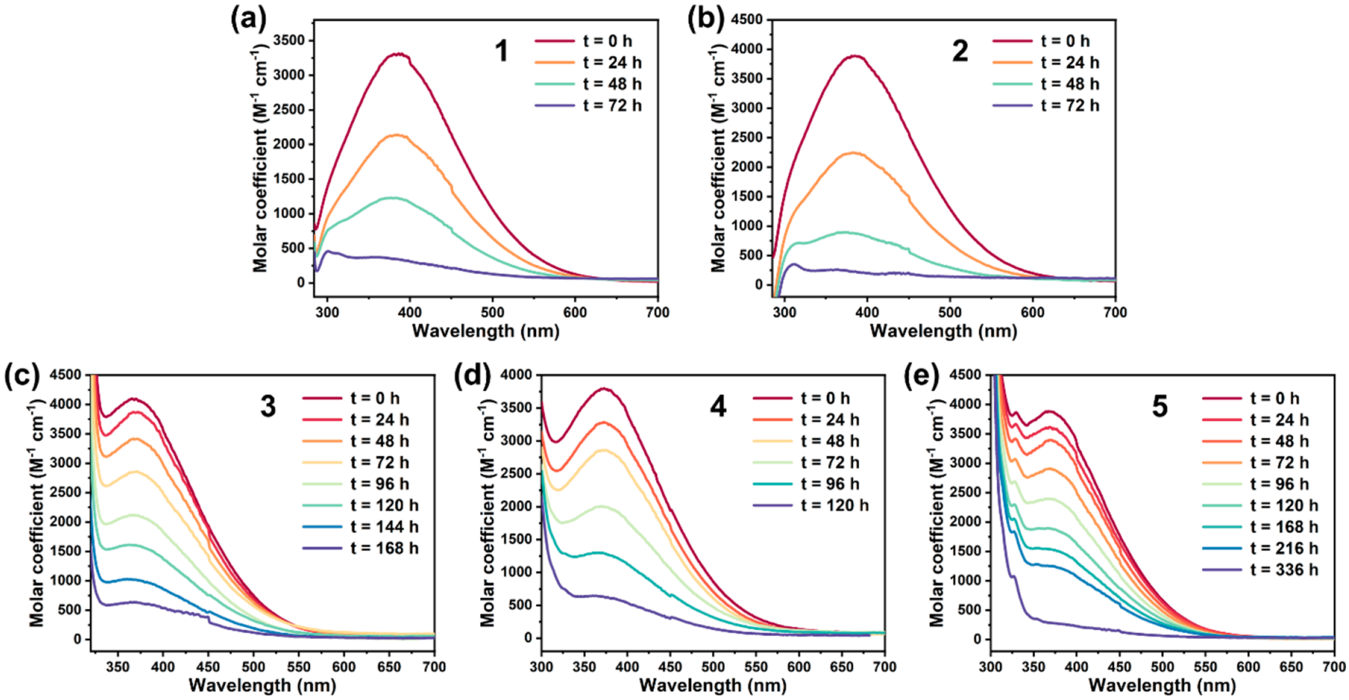

Figure 4. Time-dependent UV−vis spectra of **1**−**5** (a−e) in toluene at room temperature.

Table 4. Energies of the σ- and π-Donation from the Neutral Ligand L to the Tb(IV) Center Produced by EDA-NOCV Analysis[a]

Energy terms	1	2	3	4	5
ΔE_{int}	−49.90	−43.87	−56.54	−61.03	−62.56
$\Delta E_{orb(L \rightarrow Tb\ \sigma\ donation)}$	−23.24	−20.15	−29.62	−21.37	−27.09
$\Delta E_{orb(L \rightarrow Tb\ \pi\ donation)}$	−3.68	−4.94	−14.33	−13.26	−11.55

[a]All energies are given in kcal/mol.

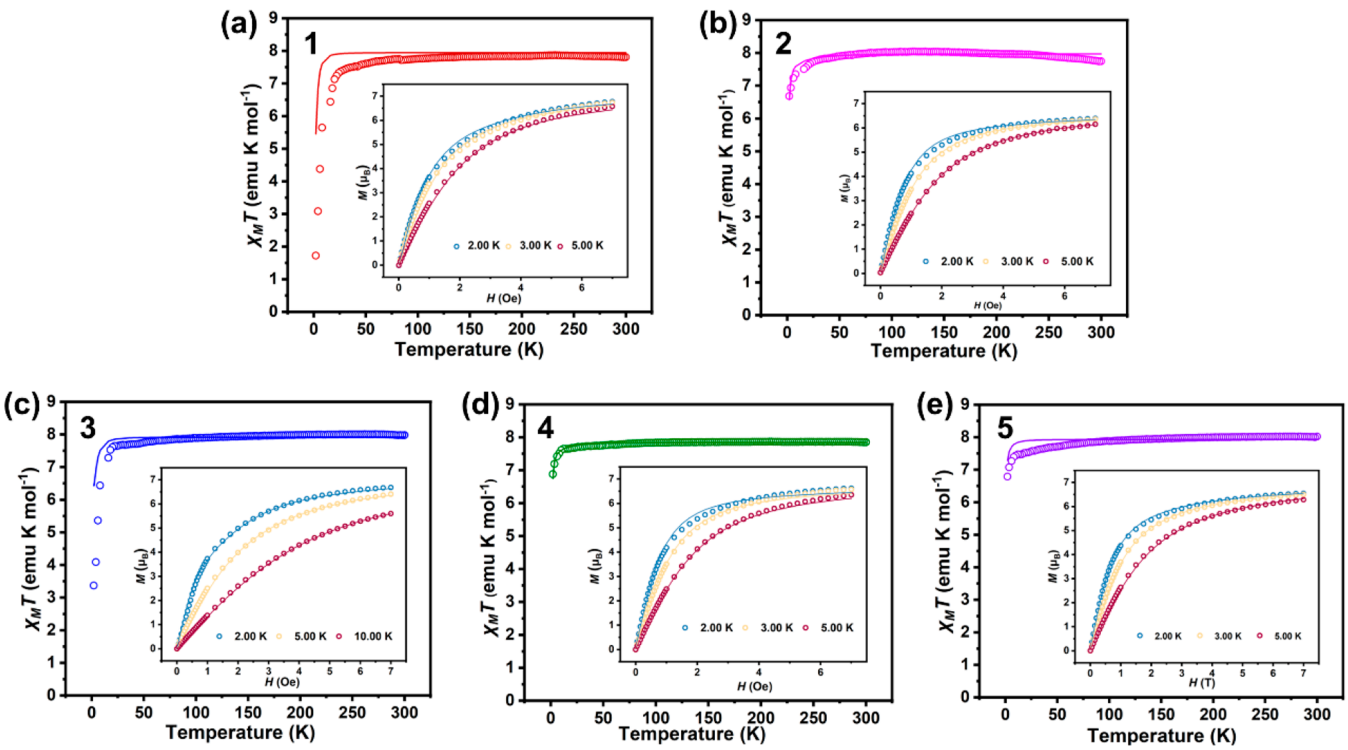

Figure 5. χT versus T plot of **1**−**5** (a-e) under 1000 Oe dc field. Inset: The field-dependent magnetization plots were at 2, 3, and 5 K. Solid lines are best fits with PHI.[60]

Table 5. Crystal Field Parameters of **1**−**5**

	Magnetization			EPR		
Complex	*g*	*D*	$\lvert E_{ZFS}\rvert$	*g*	*D*	$\lvert E_{ZFS}\rvert$
1	2.0067	−0.1103	0.0066	1.9958	0.2130	0.0040
2	2.0097	1.1484	0.0108	1.9958	0.2117	0.0043
3	2.0020	−0.1071	0.0084	1.9958	0.2100	0.0040
4	1.9953	0.7453	0.0076	1.9958	0.2050	0.0019
5	2.0060	0.4376	0.0020	1.9958	0.2127	0.0040

$\pi-\pi$ interactions, as mentioned above. It should be noted that the previously reported complexes **D** and **E** survived in a 96 h UV−vis experiment;[34] the impressive stability may be attributed, at least partly, to the shielding of the Tb(IV) center by the bulky ligands.

DFT Calculations

The bonding interactions of the Tb(IV) center with both the siloxido and neutral ligands were studied by using DFT calculations. The theoretical and computational details are given in the SI file. The metric values of Wiberg[56] and Mayer[57] bond orders obtained are collected in Table S12. The average Tb-L bond orders, ranging from 0.17 to 0.25, are much smaller than those of the Tb−$O_{siloxido}$ bonds (0.45−0.60), indicating the significant donor−acceptor character of the coordinate bond. Further analyses by EDA-NOCV[58,59] reveal the remarkable thermostability of the N-chelates (**3**−**5**) and the tuning of the Tb-L bond interactions by the chelating ligands (Table 4). For **1** and **2**, it has been found that the donation from the occupied *sp*-hybrid orbital of the THF/DME O atom to the empty 5*d* orbitals of Tb^{IV} is dominant (23.2 kcal/mol for **1**, 20.2 kcal/mol for **2**), while the π-donation is much less significant (< ∼5 kcal/mol). The opposite is, not surprisingly, observed for the N-chelates: The N-to-Tb^{IV} π-donations are found to be 14.3, 13.3, and 11.6 kcal/mol for **3**, **4**, and **5**, respectively. This difference in π donation of the neutral ligands to Tb(IV) is presumably the determining factor in the observed stability of the N-chelates with respect to their O-chelating cognates.

Magnetic Studies

The electronic structures of the complexes were further investigated by magnetic measurements and EPR. Static magnetic susceptibilities were measured under an applied DC field of 1000 Oe with cooling from 300 to 2 K (Figure 5). The χT values at 300 K are 7.81, 7.75, 7.98, 7.85, and 8.02 $cm^3\ K\ mol^{-1}$ for **1**−**5**, respectively, significantly smaller than the value of 11.82 $cm^3\ K\ mol^{-1}$ for the mononuclear Tb(III) complex but in good agreement with the values reported for other Tb(IV) complexes.[32,36] The χT decreases slowly with the lowering of temperature to ca. 20 K, at which a sudden drop occurs, reaching a minimum of 1.72, 6.68, 3.37, 6.88, and 6.79 $cm^3\ K\ mol^{-1}$ for **1**−**5**, respectively. The drop in the low-temperature region is indicative of varied zero-field splitting. Field-dependent magnetizations of complexes **1**−**5** were subsequently measured at low temperatures with the field up to a maximum of 7 T (inset in Figure 5). The maximum magnetization values at 2 K and 7 T were found to be 6.77, 6.39, 6.68, 6.62, and 6.54 μ_B for **1**−**5**, respectively, close to the saturation magnetization value of 7 μ_B calculated for the $4f^7$ electronic configuration. The temperature- and field-dependent magnetizations were fitted with the program PHI,[60] giving the isotropic Landé *g*-factor (*g*), axial zero-field splitting (*D*), and rhombic zero-field splitting (E_{ZFS}) as collected in Table 5.

Electron Paramagnetic Resonance Studies

Another important technique to evaluate the *D*, E_{ZFS}, and *g* values for magnetically active complexes is electron paramagnetic resonance (EPR) spectroscopy. The X-band (9.36 GHz) continuous-wave EPR spectra for polycrystalline samples for **1**−**5**, shown in Figure 6, were collected at 100 K. The corresponding *g* and *D* values (Table 5) were obtained via simulation.[61] While the *g* values (1.9985) are identical for all complexes, the *D* values, all around 0.2 cm^{-1}, are discernibly different. These *D*, E_{ZFS}, and *g* values, ranging from 0.1071(22) to 1.1484(112) cm^{-1}, were obtained by both fitting of the magnetization data and by EPR simulations; they are relatively small, which is consistent with the results obtained using other Tb(IV) complexes.[32,36,62]

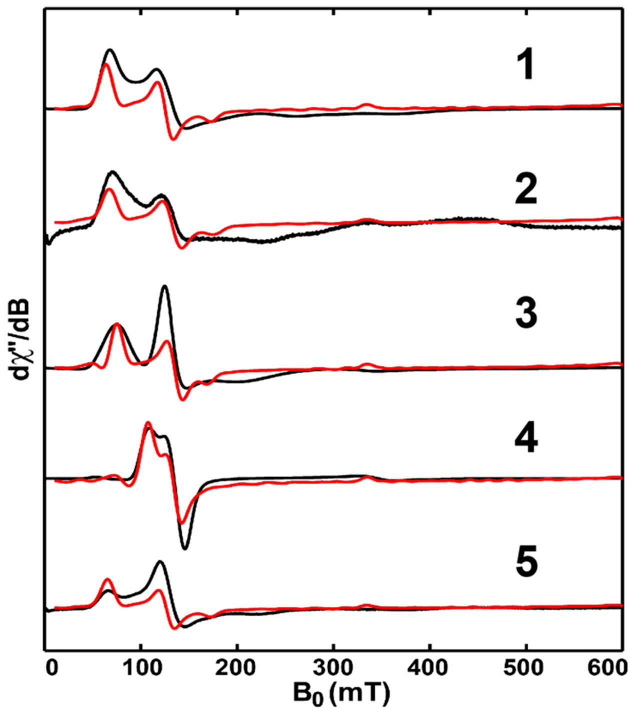

Figure 6. Experimental (black traces, measured at 9.36 GHz and 100 K) and simulated (red traces) X-band EPR spectra of solid **1**−**5**.

■ CONCLUSION

Herein, the syntheses and crystallographic structure determination of four Tb(IV) siloxido complexes with O- and N-based chelating ligands were reported together with the experimental and computational studies of their physical properties. The chelating ligands enhance the stability of the resulting complexes, as expected. More significantly, aromatic N-based chelating ligands have been found to tune effectively the electronic structures of the complexes, as evidenced by the

https://doi.org/10.1021/prechem.3c00065
Precis. Chem. 2023, 1, 583−591

sizable potential shifts observed for the quasi-reversible redox Tb(IV/III) process. Corresponding differences in the absorption spectra between the complexes in the comparison group provide further support for the tuning effect by the chelating ligands. The experimental findings are augmented with DFT calculations in which the ligand π-donation to the 5*d* orbitals of Tb(IV) center is primarily responsible for the stability enhancement and corresponding physical properties changes observed. The results by both fitting of the magnetization data and EPR simulations produced relatively small absolute values of zero-field splitting anticipated for a Tb(IV) ion situated in a distorted octahedral coordination geometry.

■ ASSOCIATED CONTENT

Supporting Information

The Supporting Information is available free of charge at https://pubs.acs.org/doi/10.1021/prechem.3c00065.

Materials and methods, synthesis, and characterization (PDF)

Crystal structures of 2267519 ($TbPh_3$), 2267520 (**1**), 2267522 (**2**), 2267521 (**3**), 2267524 (**4**), and 2267523 (**5**) (CIF)

■ AUTHOR INFORMATION

Corresponding Authors

You-Song Ding − *Department of Chemistry, Southern University of Science and Technology, Shenzhen, Guangdong 518055, China; Key University Laboratory of Rare Earth Chemistry of Guangdong, Southern University of Science and Technology, Shenzhen, Guangdong 518055, China*; Email: dingys@sustech.edu.cn

Zhiping Zheng − *Department of Chemistry, Southern University of Science and Technology, Shenzhen, Guangdong 518055, China; Key University Laboratory of Rare Earth Chemistry of Guangdong, Southern University of Science and Technology, Shenzhen, Guangdong 518055, China*; orcid.org/0000-0002-5834-6763; Email: zhengzp@sustech.edu.cn

Authors

Tianjiao Xue − *Department of Chemistry, Southern University of Science and Technology, Shenzhen, Guangdong 518055, China; Key University Laboratory of Rare Earth Chemistry of Guangdong, Southern University of Science and Technology, Shenzhen, Guangdong 518055, China*

Xue-Lian Jiang − *Department of Chemistry, Southern University of Science and Technology, Shenzhen, Guangdong 518055, China; Key University Laboratory of Rare Earth Chemistry of Guangdong, Southern University of Science and Technology, Shenzhen, Guangdong 518055, China*

Lizhi Tao − *Department of Chemistry, Southern University of Science and Technology, Shenzhen, Guangdong 518055, China*

Jun Li − *Department of Chemistry, Southern University of Science and Technology, Shenzhen, Guangdong 518055, China; Department of Chemistry and Engineering Research Center of Advanced Rare-Earth Materials of Ministry of Education, Tsinghua University, Beijing 100084, China; Key University Laboratory of Rare Earth Chemistry of Guangdong, Southern University of Science and Technology, Shenzhen, Guangdong 518055, China*; orcid.org/0000-0002-8456-3980

Complete contact information is available at: https://pubs.acs.org/10.1021/prechem.3c00065

Author Contributions

The manuscript was written through contributions of all authors. All authors have given approval to the final version of the manuscript.

Funding

This work was supported by the National Natural Science Foundation of China (92261203, 22101116, 22033005 and 21971106), Key Laboratory of Rare Earth Chemistry of Guangdong Higher Education Institutes (2022KSYS006), the Stable Support Plan Program of Shenzhen Natural Science Fund (20200925161141006), Shenzhen Fundamental Research Program (JCYJ20220530115001002), and Postdoctoral Scientific Research Fund for staying at (coming to) Shenzhen (K21217520). The calculations were performed with SUSTech supercomputer and were supported by Guangdong Provincial Key Laboratory of Catalysis (No. 2020B121201002).

Notes

The authors declare no competing financial interest.

■ ACKNOWLEDGMENTS

We thank Professor Zewei Quan for the use of the UV−vis-NIR spectrometer and Mr. Lei Li for assistance with the experiments and discussion of the results.

■ REFERENCES

(1) Martinez, J. L.; Lutz, S. A.; Yang, H.; Xie, J.; Telser, J.; Hoffman, B. M.; Carta, V.; Pink, M.; Losovyj, Y.; Smith, J. M. Structural and spectroscopic characterization of an Fe(VI) bis(imido) complex. *Science* **2020**, *370* (6514), 356−359.

(2) Wang, Z.; Lu, J.-B.; Dong, X.; Yan, Q.; Feng, X.; Hu, H.-S.; Wang, S.; Chen, J.; Li, J.; Xu, C. Ultra-Efficient Americium/Lanthanide Separation through Oxidation State Control. *J. Am. Chem. Soc.* **2022**, *144* (14), 6383−6389.

(3) Zhang, H.; Li, A.; Li, K.; Wang, Z.; Xu, X.; Wang, Y.; Sheridan, M. V.; Hu, H.-S.; Xu, C.; Alekseev, E. V.; Zhang, Z.; Yan, P.; Cao, K.; Chai, Z.; Albrecht-Schönzart, T. E.; Wang, S. Ultrafiltration separation of Am(VI)-polyoxometalate from lanthanides. *Nature* **2023**, *616* (7957), 482−487.

(4) Ungur, L. Introduction to the electronic structure, luminescence, and magnetism of lanthanides. In *Lanthanide-Based Multifunctional Materials*; Martín-Ramos, P.; Ramos Silva, M., Eds.; Elsevier: 2018; pp 1−58..

(5) Wang, Y.; Huang, W. Chemistry of non-traditional oxidation states of rare earth metals. *Sci. China Chem.* **2020**, *50* (11), 1504−1559.

(6) Su, J.; Hu, S.; Huang, W.; Zhou, M.; Li, J. On the oxidation states of metal elements in MO_3^- (M = V, Nb, Ta, Db, Pr, Gd, Pa) anions. *Sci. China Chem.* **2016**, *59* (4), 442−451.

(7) Schulz, A.; Liebman, J. F. Paradoxes and paradigms: high oxidation states and neighboring rows in the periodic table - Lanthanides, Actinides, Exotica and Explosives. *Struct. Chem.* **2008**, *19* (4), 633−635.

(8) Vent-Schmidt, T.; Riedel, S. Investigation of Praseodymium Fluorides: A Combined Matrix-Isolation and Quantum-Chemical Study. *Inorg. Chem.* **2015**, *54* (23), 11114−11120.

(9) Sroor, F. M. A.; Edelmann, F. T. Lanthanides: Tetravalent Inorganic. In *Encyclopedia of Inorganic and Bioinorganic Chemistry*; Wiley: Hoboken, NJ, 2012. DOI: 10.1002/9781119951438.eibc2034.

(10) Lucena, A. F.; Lourenço, C.; Michelini, M. C.; Rutkowski, P. X.; Carretas, J. M.; Zorz, N.; Berthon, L.; Dias, A.; Conceição Oliveira, M.; Gibson, J. K.; Marçalo, J. Synthesis and hydrolysis of gas-phase lanthanide and actinide oxide nitrate complexes: a correspondence to trivalent metal ion redox potentials and ionization energies. *Phys. Chem. Chem. Phys.* **2015**, *17* (15), 9942−9950.

(11) Hitchcock, P. B.; Lappert, M. F.; Maron, L.; Protchenko, A. V. Lanthanum Does Form Stable Molecular Compounds in the + 2 Oxidation State. *Angew. Chem. Inter. Ed.* **2008**, *47* (8), 1488−1491.

(12) Kotyk, C. M.; Fieser, M. E.; Palumbo, C. T.; Ziller, J. W.; Darago, L. E.; Long, J. R.; Furche, F.; Evans, W. J. Isolation of + 2 rare earth metal ions with three anionic carbocyclic rings: bimetallic bis(cyclopentadienyl) reduced arene complexes of La^{2+} and Ce^{2+} are four electron reductants. *Chem. Sci.* **2015**, *6* (12), 7267−7273.

(13) Fieser, M. E.; Palumbo, C. T.; La Pierre, H. S.; Halter, D. P.; Voora, V. K.; Ziller, J. W.; Furche, F.; Meyer, K.; Evans, W. J. Comparisons of lanthanide/actinide + 2 ions in a tris(aryloxide)arene coordination environment. *Chem. Sci.* **2017**, *8* (11), 7424−7433.

(14) Kelly, R. P.; Maron, L.; Scopelliti, R.; Mazzanti, M. Reduction of a Cerium(III) Siloxide Complex To Afford a Quadruple-Decker Arene-Bridged Cerium(II) Sandwich. *Angew. Chem. Inter. Ed.* **2017**, *56* (49), 15663−15666.

(15) Jenkins, T. F.; Woen, D. H.; Mohanam, L. N.; Ziller, J. W.; Furche, F.; Evans, W. J. Tetramethylcyclopentadienyl Ligands Allow Isolation of Ln(II) Ions across the Lanthanide Series in [K(2.2.2-cryptand)][$(C_5Me_4H)_3$Ln] Complexes. *Organometallics* **2018**, *37* (21), 3863−3873.

(16) Palumbo, C. T.; Darago, L. E.; Windorff, C. J.; Ziller, J. W.; Evans, W. J. Trimethylsilyl versus Bis(trimethylsilyl) Substitution in Tris(cyclopentadienyl) Complexes of La, Ce, and Pr: Comparison of Structure, Magnetic Properties, and Reactivity. *Organometallics* **2018**, *37* (6), 900−905.

(17) Palumbo, C. T.; Halter, D. P.; Voora, V. K.; Chen, G. P.; Chan, A. K.; Fieser, M. E.; Ziller, J. W.; Hieringer, W.; Furche, F.; Meyer, K.; Evans, W. J. Metal versus Ligand Reduction in Ln^{3+} Complexes of a Mesitylene-Anchored Tris(Aryloxide) Ligand. *Inorg. Chem.* **2018**, *57* (5), 2823−2833.

(18) Ryan, A. J.; Darago, L. E.; Balasubramani, S. G.; Chen, G. P.; Ziller, J. W.; Furche, F.; Long, J. R.; Evans, W. J. Synthesis, Structure, and Magnetism of Tris(amide) $[Ln\{N(SiMe_3)_2\}_3]^{1-}$ Complexes of the Non-traditional + 2 Lanthanide Ions. *Chem. -Eur. J.* **2018**, *24* (30), 7702−7709.

(19) Angadol, M. A.; Woen, D. H.; Windorff, C. J.; Ziller, J. W.; Evans, W. J. tert-Butyl(cyclopentadienyl) Ligands Will Stabilize Nontraditional + 2 Rare-Earth Metal Ions. *Organometallics* **2019**, *38* (5), 1151−1158.

(20) McClain, K. R.; Gould, C. A.; Marchiori, D. A.; Kwon, H.; Nguyen, T. T.; Rosenkoetter, K. E.; Kuzmina, D.; Tuna, F.; Britt, R. D.; Long, J. R.; Harvey, B. G. Divalent Lanthanide Metallocene Complexes with a Linear Coordination Geometry and Pronounced 6s-5d Orbital Mixing. *J. Am. Chem. Soc.* **2022**, *144* (48), 22193−22201.

(21) Anderson-Sanchez, L. M.; Yu, J. M.; Ziller, J. W.; Furche, F.; Evans, W. J. Room-Temperature Stable Ln(II) Complexes Supported by 2,6-Diadamantyl Aryloxide Ligands. *Inorg. Chem.* **2023**, *62* (2), 706−714.

(22) Moore, W. N. G.; McSorley, T. J.; Vincent, A.; Ziller, J. W.; Jauregui, L. A.; Evans, W. J. van der Waals Heterostructures Based on Nanolayered Paramagnetic Tm(II) Compounds and Boron Nitride for Investigating Spin Frustration. *ACS Appl. Nano Mater.* **2023**, *6* (8), 6461−6466.

(23) MacDonald, M. R.; Bates, J. E.; Ziller, J. W.; Furche, F.; Evans, W. J. Completing the Series of + 2 Ions for the Lanthanide Elements: Synthesis of Molecular Complexes of Pr^{2+}, Gd^{2+}, Tb^{2+}, and Lu^{2+}. *J. Am. Chem. Soc.* **2013**, *135* (26), 9857−9868.

(24) Woen, D. H.; Chen, G. P.; Ziller, J. W.; Boyle, T. J.; Furche, F.; Evans, W. J. Solution Synthesis, Structure, and CO_2 Reduction Reactivity of a Scandium(II) Complex, $\{Sc[N(SiMe_3)_2]_3\}^-$. *Angew. Chem. Inter. Ed.* **2017**, *56* (8), 2050−2053.

(25) Meihaus, K. R.; Fieser, M. E.; Corbey, J. F.; Evans, W. J.; Long, J. R. Record High Single-Ion Magnetic Moments Through $4f^n5d^1$ Electron Configurations in the Divalent Lanthanide Complexes $[(C_5H_4SiMe_3)_3Ln]^-$. *J. Am. Chem. Soc.* **2015**, *137* (31), 9855−9860.

(26) Gould, C. A.; McClain, K. R.; Yu, J. M.; Groshens, T. J.; Furche, F.; Harvey, B. G.; Long, J. R. Synthesis and Magnetism of Neutral, Linear Metallocene Complexes of Terbium(II) and Dysprosium(II). *J. Am. Chem. Soc.* **2019**, *141* (33), 12967−12973.

(27) Kundu, K.; White, J. R. K.; Moehring, S. A.; Yu, J. M.; Ziller, J. W.; Furche, F.; Evans, W. J.; Hill, S. A 9.2-GHz clock transition in a Lu(II) molecular spin qubit arising from a 3,467-MHz hyperfine interaction. *Nat. Chem.* **2022**, *14* (4), 392−397.

(28) Zhang, Q.; Hu, S.-X.; Qu, H.; Su, J.; Wang, G.; Lu, J.-B.; Chen, M.; Zhou, M.; Li, J. Pentavalent Lanthanide Compounds: Formation and Characterization of Praseodymium(V) Oxides. *Angew. Chem. Inter. Ed.* **2016**, *55* (24), 6896−6900.

(29) Hu, S.-X.; Jian, J.; Su, J.; Wu, X.; Li, J.; Zhou, M. Pentavalent lanthanide nitride-oxides: NPrO and $NPrO^-$ complexes with N≡Pr triple bonds. *Chem. Sci.* **2017**, *8* (5), 4035−4043.

(30) Gruen, D.; Koehler, W.; Katz, J. Higher Oxides of the Lanthanide Elements. Terbium Dioxide. *J. Am. Chem. Soc.* **1951**, *73*, 1475−1479.

(31) MacChesney, J.; Williams, H.; Sherwood, R.; Potter, J. Preparation and low temperature magnetic properties of the terbium oxides. *J. Chem. Phys.* **1966**, *44* (2), 596−601.

(32) Palumbo, C. T.; Zivkovic, I.; Scopelliti, R.; Mazzanti, M. Molecular complex of Tb in the + 4 oxidation state. *J. Am. Chem. Soc.* **2019**, *141* (25), 9827−9831.

(33) Willauer, A. R.; Palumbo, C. T.; Scopelliti, R.; Zivkovic, I.; Douair, I.; Maron, L.; Mazzanti, M. Stabilization of the oxidation state + IV in siloxide-supported terbium compounds. *Angew. Chem. Inter. Ed.* **2020**, *59* (9), 3549−3553.

(34) Willauer, A. R.; Douair, I.; Chauvin, A.-S.; Fadaei-Tirani, F.; Bünzli, J.-C. G.; Maron, L.; Mazzanti, M. Structure, reactivity and luminescence studies of triphenylsiloxide complexes of tetravalent lanthanides. *Chem. Sci.* **2022**, *13* (3), 681−691.

(35) Willauer, A. R.; Palumbo, C. T.; Fadaei-Tirani, F.; Zivkovic, I.; Douair, I.; Maron, L.; Mazzanti, M. Accessing the + IV Oxidation State in Molecular Complexes of Praseodymium. *J. Am. Chem. Soc.* **2020**, *142* (12), 5538−5542.

(36) Rice, N. T.; Popov, I. A.; Russo, D. R.; Bacsa, J.; Batista, E. R.; Yang, P.; Telser, J.; La Pierre, H. S. Design, isolation, and spectroscopic analysis of a tetravalent terbium complex. *J. Am. Chem. Soc.* **2019**, *141* (33), 13222−13233.

(37) Rice, N. T.; Popov, I. A.; Russo, D. R.; Gompa, T. P.; Ramanathan, A.; Bacsa, J.; Batista, E. R.; Yang, P.; La Pierre, H. S. Comparison of tetravalent cerium and terbium ions in a conserved, homoleptic imidophosphorane ligand field. *Chem. Sci.* **2020**, *11* (24), 6149−6159.

(38) Gompa, T. P.; Ramanathan, A.; Rice, N. T.; La Pierre, H. S. The chemical and physical properties of tetravalent lanthanides: Pr, Nd, Tb, and Dy. *Dalton Trans.* **2020**, *49* (45), 15945−15987.

(39) Li, N.; Zhang, W.-X. Molecular Complexes of Emerging Tetravalent Rare-Earth Metals. *Chin. J. Chem.* **2020**, *38* (11), 1449−1450.

(40) Borah, A.; Murugavel, R. Magnetic relaxation in single-ion magnets formed by less-studied lanthanide ions Ce(III), Nd(III), Gd(III), Ho(III), Tm(II/III) and Yb(III). *Coord. Chem. Rev.* **2022**, *453*, 214288.

(41) Ding, Y.-S.; Deng, Y.-F.; Zheng, Y.-Z. The Rise of Single-Ion Magnets as Spin Qubits. *Magnetochemistry* **2016**, *2* (4), 40.

(42) Liu, Z.; Wang, Y.-X.; Fang, Y.-H.; Qin, S.-X.; Wang, Z.-M.; Jiang, S.-D.; Gao, S. Electric field manipulation enhanced by strong spin-orbit coupling: promoting rare-earth ions as qubits. *Nat. Sci. Rev.* **2020**, *7* (10), 1557−1563.

(43) Hu, Z.; Dong, B.-W.; Liu, Z.; Liu, J.-J.; Su, J.; Yu, C.; Xiong, J.; Shi, D.-E.; Wang, Y.; Wang, B.-W.; Ardavan, A.; Shi, Z.; Jiang, S.-D.; Gao, S. Endohedral Metallofullerene as Molecular High Spin Qubit: Diverse Rabi Cycles in $Gd_2@C_{79}N$. *J. Am. Chem. Soc.* **2018**, *140* (3), 1123−1130.

(44) Liu, Z.; Huang, H.; Wang, Y.-X.; Dong, B.-W.; Sun, B.-Y.; Jiang, S.-D.; Gao, S. Amination of the $Gd@C_{82}$ endohedral fullerene: tunable substitution effect on quantum coherence behaviors. *Chem. Sci.* **2020**, *11* (39), 10737−10743.

https://doi.org/10.1021/prechem.3c00065
Precis. Chem. 2023, 1, 583−591

(45) McGeary, M. J.; Coan, P. S.; Folting, K.; Streib, W. E.; Caulton, K. G. Yttrium and lanthanum silyloxide complexes. *Inorg. Chem.* **1991**, *30* (8), 1723−1735.
(46) Alvarez, S.; Avnir, D.; Llunell, M.; Pinsky, M. Continuous symmetry maps and shape classification. The case of six-coordinated metal compounds. *New J. Chem.* **2002**, *26* (8), 996−1009.
(47) Yu, K.-X.; Ding, Y.-S.; Han, T.; Leng, J.-D.; Zheng, Y.-Z. Magnetic relaxations in four-coordinate Dy(iii) complexes: effects of anionic surroundings and short Dy-O bonds. *Inorg. Chem. Fron.* **2016**, *3* (8), 1028−1034.
(48) Petersen, J. B.; Ding, Y.-S.; Gupta, S.; Borah, A.; McInnes, E. J. L.; Zheng, Y.-Z.; Murugavel, R.; Winpenny, R. E. P. Electron Paramagnetic Resonance Spectra of Pentagonal Bipyramidal Gadolinium Complexes. *Inorg. Chem.* **2023**, *62* (21), 8435−8441.
(49) Hirneise, L.; Langmann, J.; Zitzer, G.; Ude, L.; Maichle-Mössmer, C.; Scherer, W.; Speiser, B.; Anwander, R. Tuning Organocerium Electrochemical Potentials by Extending Tris-(cyclopentadienyl) Scaffolds with Terminal Halogenido, Siloxy, and Alkoxy Ligands. *Organometallics* **2021**, *40* (11), 1786−1800.
(50) Friedrich, J.; Qiao, Y.; Maichle-Mössmer, C.; Schelter, E. J.; Anwander, R. Redox-enhanced hemilability of a tris(tert-butoxy)siloxy ligand at cerium. *Dalton Trans.* **2018**, *47* (30), 10113−10123.
(51) Bogart, J. A.; Lippincott, C. A.; Carroll, P. J.; Booth, C. H.; Schelter, E. J. Controlled Redox Chemistry at Cerium within a Tripodal Nitroxide Ligand Framework. *Chem.—Eur. J.* **2015**, *21* (49), 17850−17859.
(52) Hobart, D. E.; Samhoun, K.; Young, J. P.; Norvell, V. E.; Mamantov, G.; Peterson, J. R. Stabilization of praseodymium(IV) and terbium(IV) in aqueous carbonate solution. *Inorg. Nucl. Chem. Lett.* **1980**, *16* (5), 321−328.
(53) Hoefdraad, H. E. Charge-transfer spectra of tetravalent lanthanide ions in oxides. *J. Inorg. Nucl. Chem.* **1975**, *37* (9), 1917−1921.
(54) Gritsenko, O. V.; Schipper, P. R. T.; Baerends, E. J. Approximation of the exchange-correlation Kohn-Sham potential with a statistical average of different orbital model potentials. *Chem. Phys. Lett.* **1999**, *302* (3), 199−207.
(55) Kinnunen, T.-J. J.; Haukka, M.; Nousiainen, M.; Patrikka, A.; Pakkanen, T. A. Electron withdrawing and electron donating effects of 4,4′-bipyridine substituents on ruthenium mono(bipyridine) complexes. *J. Chem. Soc., Dalton Trans.* **2001**, No. 18, 2649−2654.
(56) Wiberg, K. B. Application of the pople-santry-segal CNDO method to the cyclopropylcarbinyl and cyclobutyl cation and to bicyclobutane. *Tetrahedron* **1968**, *24* (3), 1083−1096.
(57) Mayer, I. Charge, bond order and valence in the AB initio SCF theory. *Chem. Phys. Lett.* **1983**, *97* (3), 270−274.
(58) Michalak, A.; Mitoraj, M.; Ziegler, T. Bond Orbitals from Chemical Valence Theory. *J. Phys. Chem. A* **2008**, *112* (9), 1933−1939.
(59) Mitoraj, M. P.; Michalak, A.; Ziegler, T. A Combined Charge and Energy Decomposition Scheme for Bond Analysis. *J. Chem. Theory Comput.* **2009**, *5* (4), 962−975.
(60) Chilton, N. F.; Anderson, R. P.; Turner, L. D.; Soncini, A.; Murray, K. S. PHI: A powerful new program for the analysis of anisotropic monomeric and exchange-coupled polynuclear d- and f-block complexes. *J. Comput. Chem.* **2013**, *34* (13), 1164−1175.
(61) Stoll, S.; Schweiger, A. EasySpin, a comprehensive software package for spectral simulation and analysis in EPR. *J. Magn. Reson.* **2006**, *178* (1), 42−55.
(62) Gompa, T. P.; Greer, S. M.; Rice, N. T.; Jiang, N.; Telser, J.; Ozarowski, A.; Stein, B. W.; La Pierre, H. S. High-Frequency and -Field Electron Paramagnetic Resonance Spectroscopic Analysis of Metal-Ligand Covalency in a $4f^7$ Valence Series (Eu^{2+}, Gd^{3+}, and Tb^{4+}). *Inorg. Chem.* **2021**, *60* (12), 9064−9073.

https://doi.org/10.1021/prechem.3c00065
Precis. Chem. 2023, 1, 583−591